

# Road Cycling Time Trial Strategy via Joint Simulation

## Summary

The competition strategy plays an extremely important role in the road bicycle **time trial**. It is affected by various factors. In this paper, we focus on the optimization of the model through simulation to achieve the optimal lap time under the condition of balancing energy and power.

For Task 1, We used the hyperbolic sine to fit the power curve data of cyclists of different types and genders, and found the hyperbolic sine fits very well. The result is Function [15]. We combined the hyperbolic sine and **Skiba Energy Store Model** to quantify **Energy Consumption Model** of our riders. Then we defined the time trial specialist and sprinter the power curve, and get the Critical Power (CP) according to the power curve, and then define their parameters in Skiba Energy Store Model to get their power profile.

For Task 2, we built our **Power Distribution Model**(PDM) based on the energy model from Task 1. The results of the linear combination of the circuit parameters are passed into the **sigmoid** as the decay factor of the maximum output power. Then, we analyzed the force and motion of the bicycle and listed the differential equations of the bicycle motion. In addition, we collected and post-processed the data of **Circuit Model** to obtain some characteristics of them. We then combined these four Models to form a closed-loop control chain[3]. We used the **PSO** to optimize the parameters of the model. The final lap time of Time Trial Specialist we obtained referred to **Table 6**.

For Task 3, taking the UCI Flanders as an example, we take the effect of wind speed, wind direction, altitude and temperature into account. For wind speed and wind direction, we further improved the **Kinematic Bicycle Model** based on the model from Task 2 by introducing two variables: wind speed and the angle between the direction of travel. When the wind speed range from 0 to 20kph, the Lap time increased from 62.47 to 66.53 minutes. Meanwhile, when the wind direction is changed by 25%, the lap time will change by 1.7% on average. In terms of altitude and air temperature, the air density can be obtained from the ideal gas equation of state, and the air density can be directly reflected in the air resistance. For every 1000m increase in Altitude, the lap time increases by an average of 2.06 minutes. The effect of temperature on lap time is on average 0.88% for every 1% change in temperature from 273.15K.

For Task 4, taking the UCI Flanders as an example, we further improve the PDM based on previous tasks by introducing a uniformly distributed random number and converting it to the power output of the rider to examine the robustness and sensitivity of the overall motion system. The final result is no impact.

For Task 5, taking the UCI Flanders as an example we searched for information about team road cycling time trials and summarized two important variables, i.e., alternate wind ride-in-a-paceline and final sprint distance, and added them into our model to extend the model to team time trials. The final result is that the wind ride-in-a-paceline for the four sprinters is 25s , the other two alternate wind ride-in-a-paceline is 40s, and the final sprint distance is 40km , and the total time of the team race will be about 530seconds faster compared to the individual time trial race.

**Keywords:** Skiba Energy Store Model; Kinematic Bicycle Model; PSO; Circuit Model

## Contents

<b>1</b>	<b>Introduction</b>	<b>2</b>
1.1	Problem Background . . . . .	2
1.2	Restatement of the Problem . . . . .	2
1.3	Literature Review . . . . .	3
1.4	Our Work . . . . .	3
<b>2</b>	<b>Asssumptions</b>	<b>3</b>
<b>3</b>	<b>Notations</b>	<b>4</b>
<b>4</b>	<b>Establishment of Our Control Model</b>	<b>5</b>
4.1	Kinematic Bicycle Model . . . . .	5
4.2	Energy Consumption Model . . . . .	9
4.3	Power Distribution Model . . . . .	11
4.4	Circuit Model . . . . .	12
4.5	Simulation Results . . . . .	14
<b>5</b>	<b>Influences of Weather and Environment</b>	<b>14</b>
5.1	Wind Strength and Wind Direction Influences . . . . .	14
5.2	Altitude and Temperature Influences . . . . .	15
<b>6</b>	<b>Sensitivity Analysis of Power Distribution Model</b>	<b>17</b>
6.1	Adjustments to Power Distribution Models . . . . .	17
6.2	Analysis of Results . . . . .	17
<b>7</b>	<b>Extension and Optimization of Our Model</b>	<b>18</b>
7.1	Discussion on Team Strategies . . . . .	19
7.2	Optimization of Our Model . . . . .	19
7.3	Analysis of Results . . . . .	19
<b>8</b>	<b>Strengths, Weaknesses and Further Improvements</b>	<b>20</b>
8.1	Strengths . . . . .	20
8.2	Weaknesses and Further Improvements . . . . .	21
	<b>Race Guidence</b>	<b>23</b>

# 1 Introduction

## 1.1 Problem Background

Anna Kiesenhofer won the gold medal in the women's individual road race at the Tokyo Olympics. Meanwhile, she is a postdoctoral researcher at the Ecole Polytechnique Fédérale de Lausanne(EPFL).



**Figure 1:** Anna Kiesenhofer, the champion in the women's road race at the Tokyo Olympics (from the website <https://cyclingtips.com/>)

Obviously, she didn't win the gold medal by talent or luck. She said that she did research on the course before the race, and analyzed her body data, and she used cycling data to analyze her body functions. It can be seen that scientific analyses have a terrific effect on the results of the cyclists' race. Among them for road cyclists, the power distribution on the entire route has attracted much attention. Better use of power means more efficient completion of the race, which means they can finish the race within less time. So we need to figure out the Power Profile of cyclists to help them get better performance.

## 1.2 Restatement of the Problem

- Build a mathematical model to describe the rider's power distribution curve, while the rider has a certain power ceiling, has the ability to recover power, and should accumulate fatigue during the race. Some variadic parameters in the model control some of the rider's attributes, such as gender, type and so on. With the cyclist model, optimal power distribution for the rider in different courses can be predicted.
- Collect and analyze the data about the chosen race courses. Latitude, longitude, altitude and other details are processed into various physical quantities that can be used to study the impact of complex road sections, such as uphill and downhill, sharp turns on the rider's power output. In addition, the model will be applied to at least three courses mentioned in the requirements. On this basis, we can not only analyze the characteristics of a particular track, but also quickly determine the power distribution of different players on different tracks.
- Consider more factors that may have effects on our model, such as wind direction, wind strength, ambient pressure, temperature and altitude and so on. The track information should be fully processes and utilized. In this way, our model will have a wider range of applications and be more robust and convincing.

- Analyze the sensitivity of the model on unplanned power output of the cyclist. Study the effects on the power distribution in the whole course and the race results. For the needs of the rider and the Directeur Sportif, the solution will be given in the rider's guide.
- Figure out the difference between team and individual races. Make further exploration of the scalability and adaptability of our model when used in team race or other different situations.

## 1.3 Literature Review

Training and racing with mobile power meter for bicycles is now standard practice in a wide range of cycling disciplines. This allows athletes and coaching teams to accurately record power output data in real time under live conditions. Researchers can analyse the athlete's data in depth based on the power output. (Passfeld et al. 2017). The invention of these techniques has made cycling motion analysis a popular area of research, with its inclusion of real-time measurements of internal (e.g. heart rate) and external (e.g. power output) workloads (van Erp and de Koning 2019; Muriel et al. 2021). This in turn allows coaching teams to train athletes according to the requirements of the competition (van Erp et al. 2021b; Menaspà et al. 2015). To date, however, there is no clear answer to the question of what constitutes the optimal race strategy, and many new research questions and practical approaches are emerging. Our work will focus on power allocation by developing a relevant model and optimizing it, with the aim of improving race performance in specific race conditions.

## 1.4 Our Work

We have drawn a detailed block diagram to summarize our work, as **Figure 2** shows.

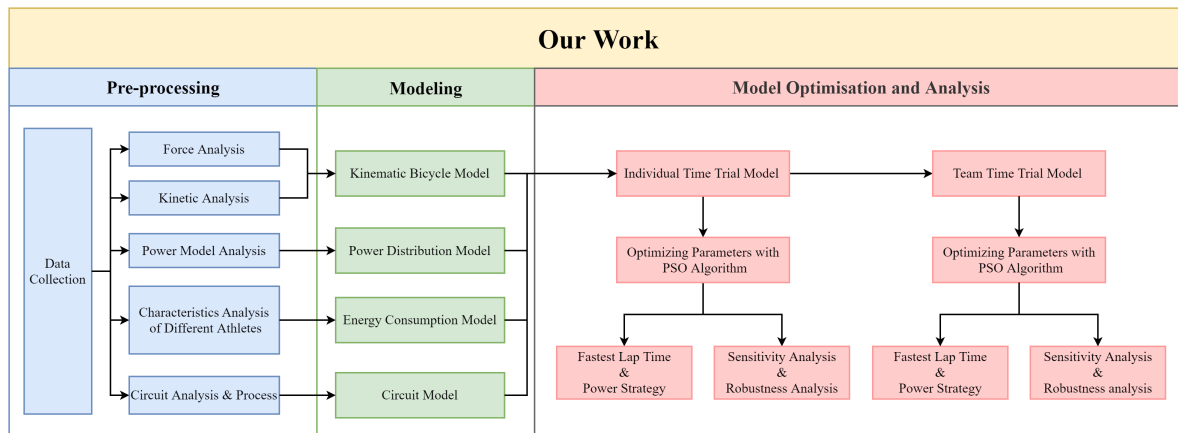


**Figure 2:** Our Work

## 2 Assumptions

- Assumption 1** The expenditure of  $W'$  begins when the athlete exceeds  $CP$ .
- Assumption 2** The energy balance begins to increase again when the athlete falls below  $CP$ .
- Assumption 3** the reconstitution of  $W'$  follows an exponential time recovery path which weights recent efforts more heavily than efforts further back in time.

- **Assumption 4** *The bicycle has less deformability.* The frame is generally made of carbon fiber, so the bicycle generally has high frame rigidity and strength.
- **Assumption 5** *Ignore the small deformation and lateral deflection characteristics of the tire.* Race tires with high tire pressure and narrow tread.
- **Assumption 6** *Ignore the slip of the drive wheel, i.e. the slip rate is zero.* The applied torque is small enough to ignore slippage.
- **Assumption 7** *Ignore the physical and psychological effects of the environment on riders.* This varies from person to person, so it's difficult to quantify.
- **Assumption 8** *Default that rider selects the fastest path to travel.*

### 3 Notations

The key mathematical notations used in this paper are listed in **Table 1 and 2**. In general, symbols with the same capital but different subscripts indicate the variables with similar physical properties. **Note:** Some local variables are not listed here, but will be discussed in detail in each section.

**Table 1: Notations used in this paper**

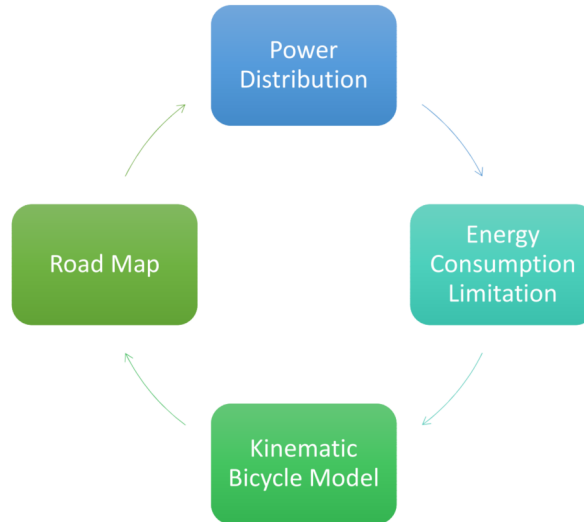
Symbol	Description
$CP$	critical power
$\tau$	time constant that indicates the recovery capability of the cyclist
$\delta$	mass conversion coefficient
$m$	overall mass of the bicycle and the rider
$r$	the radius of the bicycle wheel
$i_g$	gear ratio
$\mu$	rolling friction coefficient
$A$	windward area
$C_D$	air resistance coefficient
$r_{brk}$	the radius of the braking plate
$\phi$	peak ground adhesion coefficient
$u_x, u_w$	longitudinal vehicle speed and longitudinal wind speed
$g$	gravitational constant
$F_t, T_{toq}$	driving force and torque
$P$	power
$n_w, n_{fw}$	rotational speed of wheel and fly wheel
$\eta$	mechanical drive efficiency
$F_w, F_{win}, F_{wex}$	air resistance
$F_x$	driving resistance
$F_G$	slope resistance
$F_{brk}, T_{brk}$	braking force and torque

**Table 2: Notations used in this paper**

Symbol	Description
$F_Z$	vertical force
$\aleph$	slope
$R$	Turning radius
$\beta$	the angle between the wind and the bicycle's direction
$W'$	total energy
$W'_{bal}$	residual energy
$k_1, k_2, k_3, k_4$	parameters of PDM

## 4 Establishment of Our Control Model

The **Figure 3** describes the overall control strategy of the model.

**Figure 3:** Control Strategy

### 4.1 Kinematic Bicycle Model

#### 4.1.1 Overview of Forces on The Whole Bicycle

First of all, we need to determine the kinematic of the bicycle, i.e. to determine the movement of the bicycle along the direction of travel. To this end, we need to grasp the various external forces acting along the direction of the bicycle, i.e. the driving force and the running resistance. Based on the equilibrium inertia of these forces, we can further estimate the acceleration and velocity of the bicycle as well as the distance travelled. It can be analyzed that the bicycle is roughly subjected to the following forces in the direction of travel: human driving moment on the pedals, rolling resistance, air resistance, and grade resistance (**Figure 4** shows the motion on flat ground). The following is a specific force analysis of the tire. In the case of neglecting the rolling characteristics of the small tire deformation, the driving wheel is mainly subjected to

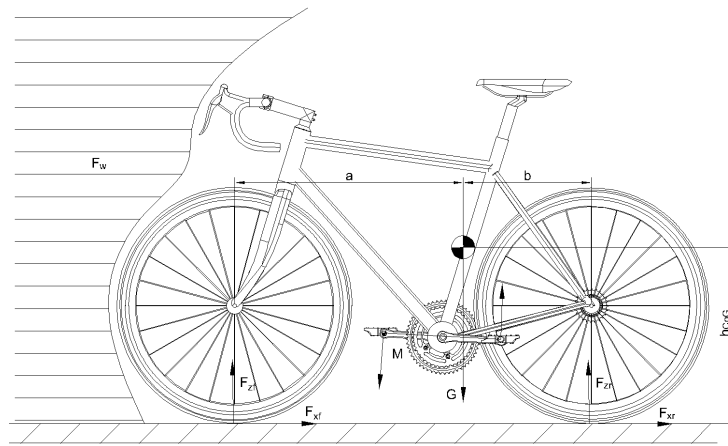


**Figure 4:** Force analysis diagram of the bicycle model

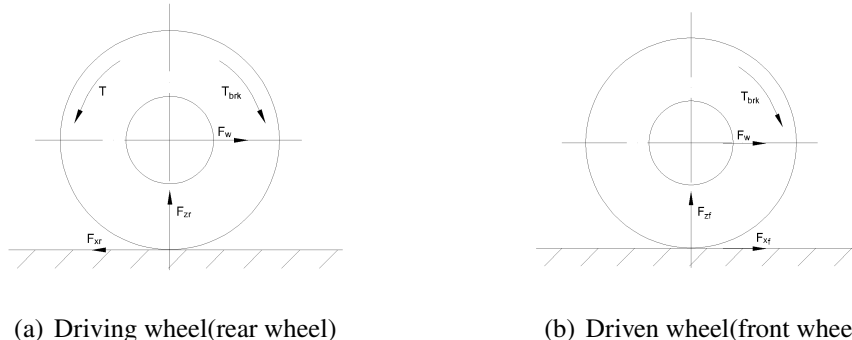


**Figure 5:** Driving and driven wheel

the driving moment, braking moment and the reaction force of the road on it. The driven wheel is mainly subjected to the braking moment and the reaction force of the road surface.(As shown in **Figure 5.**) In order to further simplify the model, we set the center of mass of the bike as the center of mass of the front and rear wheels, while moving the air resistance point to the new center of mass, and introducing a mass conversion coefficient  $\delta$  to offset the effects of various types of rotational moments. The formula for calculating  $\delta$  is as follows:

$$\delta = 1 + \frac{\sum I_w}{r^2} + \frac{I_f i_g^2 \eta}{mr^2} \quad (1)$$

where  $I_w$  is the rotational inertia of the wheel, and  $I_f$  is the rotational inertia of the flywheel. So far, we can list the differential equation of longitudinal motion of the bicycle according to Newton's second law:

$$\delta m \frac{du_x}{dt} = F_t - F_{win} - F_{wex} - F_x - F_G - F_{brk} \quad (2)$$

### 4.1.2 Driving Force

First we have to calculate the torque applied by the person on the pedal according to its applied power, and convert it to the rear wheel.

$$T_{Flywheel} = 9550 \frac{P}{n_{Flywheel}} \quad (3)$$

$$i_g = \frac{n_{Flywheel}}{n_{wheel}} \quad (4)$$

$$T_{toq} = T_{Flywheel} \cdot i_g \quad (5)$$

With the driving moment, the driving moment generates a pair of circumferential forces on the ground, and the ground will also have a reaction force  $F_t$  on the driving wheel, which is the external force driving the car. The calculation formula is as follows, which needs to be explained is that the radius of rotation of the tire can be considered as the radius of the wheel.

$$F_t = \frac{T_{toq} i_g \eta}{r_r} \quad (6)$$

where  $r_r \approx r$ .

### 4.1.3 Rolling Resistance and Slope Resistance

Rolling resistance refers to the normal and tangential interaction forces generated in the contact area between the tire and the road surface when the wheel rolls. In order to avoid analyzing the tires' moment of rolling resistance couple which is too complicated, we reviewed the data [2] and decided to quantify it using the following equation.

$$F_x = \mu mg \cos \alpha \quad (7)$$

The slope resistance refers to the component force of the bike's gravity along the slope when the bike travels uphill or downhill. Its calculation formula can be solved through force analysis, as the following formula shows:

$$F_G = m g \sin \alpha \quad (8)$$

### 4.1.4 Air Resistance

When driving in a straight line, the component of the air forcing on the bicycle in the direction of travel is called air resistance. Air resistance can be divided into two parts: pressure resistance and friction resistance. Within the driving range of the bicycle, the value of air resistance is usually summed up in a form that is proportional to the dynamic pressure  $\frac{1}{2} \rho u_x^2$  of the relative velocity of the airflow[2]. The specific formula is as follows:

$$F_w = F_{win} = \frac{1}{2} C_D A \rho u_x^2 \quad (9)$$

where  $C_D$  is the air resistance coefficient, which is generally a function of Reynolds number  $Re$ . At higher vehicle speeds, higher dynamic pressures and lower corresponding gas viscous friction,  $C_D$  can be assumed not to vary with  $Re$ .

#### 4.1.5 Braking Force

The braking torque refers to the friction torque when the friction plate in the wheel brake slides against the brake disc. The braking torque and the longitudinal force of the ground on the wheel can be calculated according to the following formula:

$$T_{brk} = \mu_{brk} F_r r_{brk} \quad (10)$$

where  $\mu_{brk}$  is the sliding friction coefficient of the brake pad and the brake disc.

$$F_{brk} = \frac{T_{brk}}{r_r} \quad (11)$$

At the same time, there is a certain relationship among the ground braking force, the brake braking force and the adhesion force, i.e. the ground braking force is the binding reaction force of sliding friction, and its value cannot exceed the adhesion force. We can calculate the maximum ground braking force[2]:

$$F_{brk} \leq F_\varphi = F_Z \varphi \quad (12)$$

where  $F_\varphi$  is the wheel adhesion.

$$F_{brkmax} = F_Z \varphi \quad (13)$$

Since it is a time trial, we always hope to maximize the braking efficiency, so we ignore the calculation process of the braking torque and directly estimate the ground braking force based on 90% of the maximum force.

#### 4.1.6 Transmission

Road bikes are often equipped with derailleurs. In terms of power, a reasonable selection of gears can maximize the power advantage and improve performance. As far as physical fitness is concerned, a reasonable selection of gears can also save physical power consumption. In terms of gear selection, the transmission ratio of each gear is generally distributed according to the proportional sequence. Taking the Cervelo P-Series 105 road bike selected in this article as an example, the gearbox used is Shimano 105 R7000 with 34T-50T teeth and 0.68-1.47 gear ratio. We finally chose seven of them, i.e. the seven-speed transmission. The gear ratio information of each gear is as follows:

**Table 3:** Gear ratio for each gear of the transmission

Gears	1	2	3	4	5	6	7
Gear ratio	1.47	1.27	1.15	1	0.86	0.78	0.68

We made a graph of the relationship between the speed of each gear and the speed of the pedal flywheel as follows.

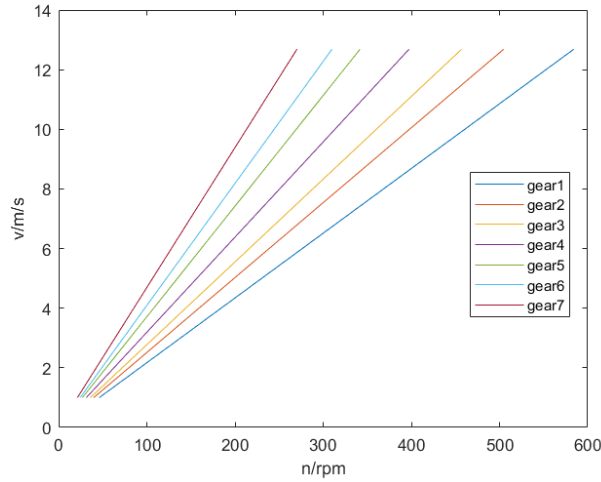


**Figure 6:** the relationship between the speed of each gear and the speed of the pedal flywheel

And the shifting timing is selected, that is, upshifting greater than 270rpm and downshifting less than 200rpm, in order to maintain a reasonable power output continuously and save energy to a certain extent. The calculation formula of shifting timing is as follows[2]:

$$\frac{n_1}{i_{g2}} = \frac{n_2}{i_{g1}} \quad (14)$$

where  $n$  is the speed of the flywheel and  $i_g$  is the gear ratio of each gear.

## 4.2 Energy Consumption Model

### 4.2.1 Power Curve

Critical power CP is the maximum power level, in watts, that a cyclist can sustain over a given period of time. Each power level and its corresponding time constitute a power curve. It was discussed in the paper '*Optimizing Cycling Power*'[1] that, the shape of the power curve generally follows the hyperbolic curve, where time is along the X-axis and power is along the Y-axis.

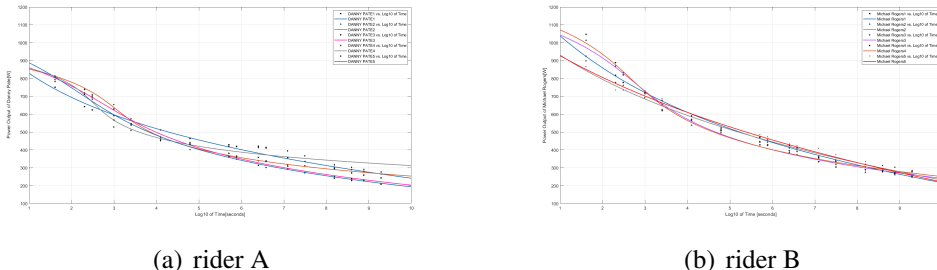


**Figure 7:** Different professional riders' power curve plotted with the data on the website[8]

$$f(x) = a \cdot \operatorname{arcsinh}(b \cdot \log_{10}(x) + c) + d \quad (15)$$

We collected a number of data points from the website[8] that could characterize the power curve of the cyclists, and we fit them with the **Function 15** and find that the fit is quite good, as shown in **Figure 7**. Power curve indicates that cyclists can maintain extremely high power levels for short periods of time (e.g., during the sprint phase), while they can maintain relatively low power levels for longer periods of time.

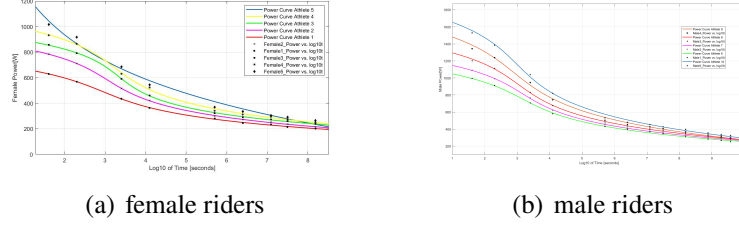


**Figure 8:** Power curve of riders' of different types and genders

According to **Figure 7** and **Figure 8**, it's obvious that the power curve varies from rider to rider. We analyze the power curve of different types of cyclists with similar levels. Riders with strong explosive power, such as the Sprinter, are able to deliver especially high power in a short period of time. Riders with strong endurance, such as individual time trial riders, are able to maintain a higher power output even after a longer period of time. As shown in [Figure 8 (a)], the blue line stands for the rider whose ability is quite like a sprinter, while the grey one cannot sprint that fast during a short period of time, but he maintain higher power output after about 1.5 hours. Certainly, we cannot neglect the difference between female and male. Male riders usually have a better overall physical fitness than female ones, which also shown in the Figure. Cyclists often use functional threshold power (FTP) to describe their CP rather than a power curve. FTP is the average maximum power output a cyclist can sustain over a one-hour period.

#### 4.2.2 Skiba Energy Store Model

In the Skiba Energy Store Model[7],  $W'$  characterizes the ability to do work beyond a critical power.  $W'$  can be obtained from power,  $CP$  and time, where  $CP \approx 95\%$  FTP.

$$P = \left( \frac{W'}{t} \right) + CP \quad (16)$$

The model makes three assumptions. The assumptions have been mentioned in Chapter 2.  $W'_{bal}$  represents the remaining amount of  $W'$ , which can be calculated according to the following formula:

$$W'_{bal} = W' - \int_0^t W'_{exp}(u) e^{-\frac{(t-u)}{\tau_W}} du \quad (17)$$

$\tau$  characterizes an rider's ability to recover. For riders of similar ability, the  $\tau$  of a sprinter is slightly smaller than that of an individual time-trial rider.

#### 4.2.3 Power Profile

We have designed the energy parameters for two types of cyclists, the sprinter and the individual time-trial runner, one male and one female for each type. Their curve are shown in the Table below. We assumed the same energy  $W_{total}$  for the same type of riders of the same gender and set the appropriate values based on the information consulted. We defined the hyperbolic function shown in the table below as the power curve and obtained and CP. Power profile is shown in **Table 5**.

**Table 4:** function of different types

type	male	female
sprinter	$290.5 \operatorname{arcsinh}(-1.213 \log_{10}(x) + 3.063) + 1061$	$158.3 \operatorname{arcsinh}(-1.514 \log_{10}(x) + 4.902) + 677.2$
time trial specialist	$186.9 \operatorname{arcsinh}(-1.067 \log_{10}(x) + 3.37) + 755$	$134.4 \operatorname{arcsinh}(-1.472 \log_{10}(x) + 4.503) + 490$

**Table 5:** Power Profile

Type	Gender	$W'_{total}(J)$	$CP(W)$	$\tau$
time trial specialist	male	5000	250	375
	female	5000	210	465
sprinter	male	4000	190	482
	female	4000	170	523

## 4.3 Power Distribution Model

### 4.3.1 PDM

Our power distribution model manages to achieve the fastest lap timewhile balancing energy and power output. Considering that the slope and turning radius in the terrain of the actual track and the fatigue degree of the human body gradually increase with time, we adopt the slope, radius and time as the variables of the energy distribution model.

Based on physiological data, we found that many motion-related curves in the human body are similar in shape to hyperbolic functions. In addition, they have strong nonlinear characteristics, but are significantly different from quadratic or cubic power functions. We abandoned hyperbolic functions such as  $\sinh$ , and simplified the use of  $\text{sigmoid}$  to make our model from linear to nonlinear, and its upper and lower bounds can be controlled within a certain range.

We refer to the principle of a single-layer neural network, simply linearly combine the radius  $r$  of the track, the time of the movement, and add a bias  $k_4$ , which is combined with the sigmoid function to obtain the following formula:

$$P = \left( \frac{1}{1 + e^{k_1 R + k_2 s + k_3 t + k_4}} \right) \cdot P_{max} \quad (18)$$

where  $P_{max}$  is the maximum power that can be consumed.

According to the principle of neural network, *PDM* has better fitting ability to approach our realistic power distribution strategy. Since the sigmoid range is  $(0, 1)$ , the power distributed will neither be 0 nor exceed the maximum power that the rider can distribute.

### 4.3.2 PSO-PDM Optimization

Since the specific parameters in the *PDM* model are obviously related to the rider's own energy attributes and each track, to use the *PDM* model to obtain a good energy allocation strategy, we need to optimize the parameters of the *PDM*. Our *PDM* solution can be expressed as:

$$\begin{aligned} \min \quad & t(k_1, k_2, k_3, k_4), k_1, k_2, k_3, k_4 \in R \\ g(x) = -W'_{total} \leq 0 \end{aligned} \quad (19)$$

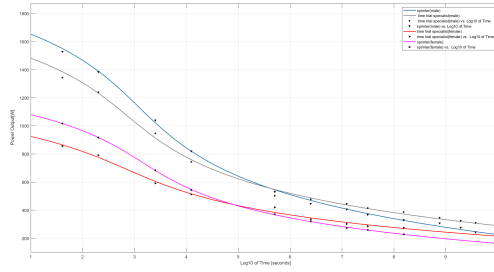


**Figure 9:** Power Profile

We optimize the parameters of the *PDM* model through particle swarm optimization, and the PSO algorithm is shown in **Algorithm 1**. Since PSO is not suitable for solving constrained problems, we transform the problem into unconstrained optimization and express as follows:

$$F(x) = f(x) + h(k)H(x) \quad (20)$$

$$h(k) = k\sqrt{k} \quad (21)$$

$$H(x) = \theta(q(x))(q(x))^{r(q(x))} \quad (22)$$

where  $q(x)$  is relative constraint penalty function,  $\theta(q(x))$  is segment penalty function,  $r(q(x))$  is penalty function.

---

#### Algorithm 1: Particle Swarm Optimization(PSO)

---

**Input:** road model  $M_{road}$ , particle number  $N$ , iteration number  $T$ , dimension  $D$

**Output:** Optimal particle  $gBest$

```

1 Initialize velocity  $v_{id}$ ,position  $x_{id}$  randomly within permissible range;
2  $gBest = \min\{pBest_i\}$ , Iteration  $k = 1$ ;
3 while maximum iteration or minimum error criteria are not attained do
4   for  $i = 0$  to  $N - 1$  do
5     Calculate fitness value for particle  $i$  based on  $M_{road}$ ;
6     if the fitness value fit is better than  $pBest_i$  in history then
7       | Set current fitness as  $pBest_i$ ;
8     end
9     if the fitness value fit is better than  $gBest$  then
10      | Set current fitness as  $gBest$ ;
11    end
12  end
13  Update particle position according to the equation;
14   $k = k + 1$ ;
15 end

```

---

#### 4.4 Circuit Model

We tested the performance of our model by applying the model to the 2021 Olympic Time Trial course in Tokyo, Japan, the 2021 UCI World Championship time trial course in Flanders, Belgium, and our own designed course. The length of 2021 Olympic Time Trial course is 22km. The length of the 2021 UCI World Championship time trial course in Flanders is 44km. The length of our own designed course is 7km.

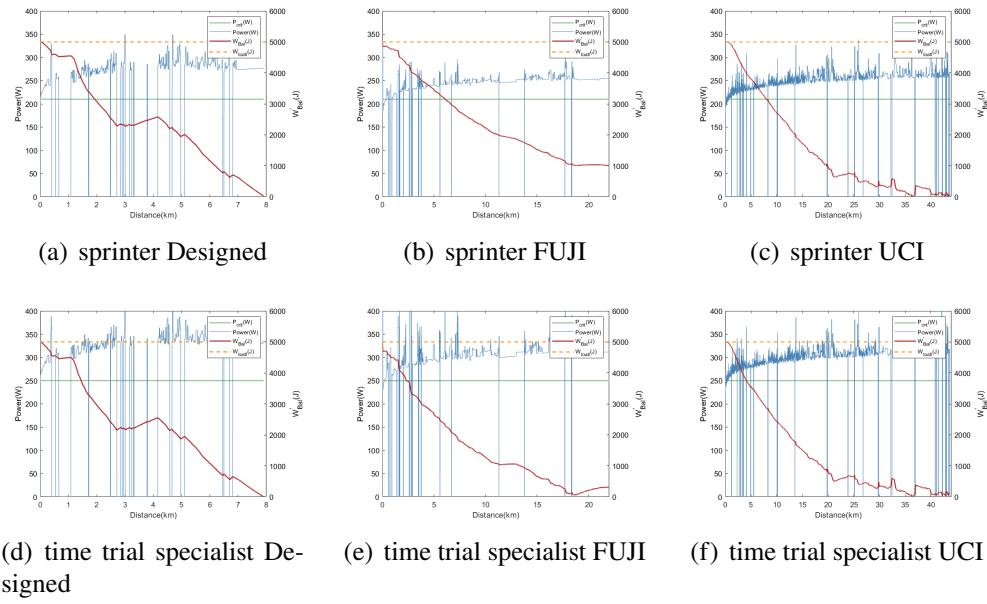


**Figure 10:** Time trial specialist and sprinter's performance in three courses

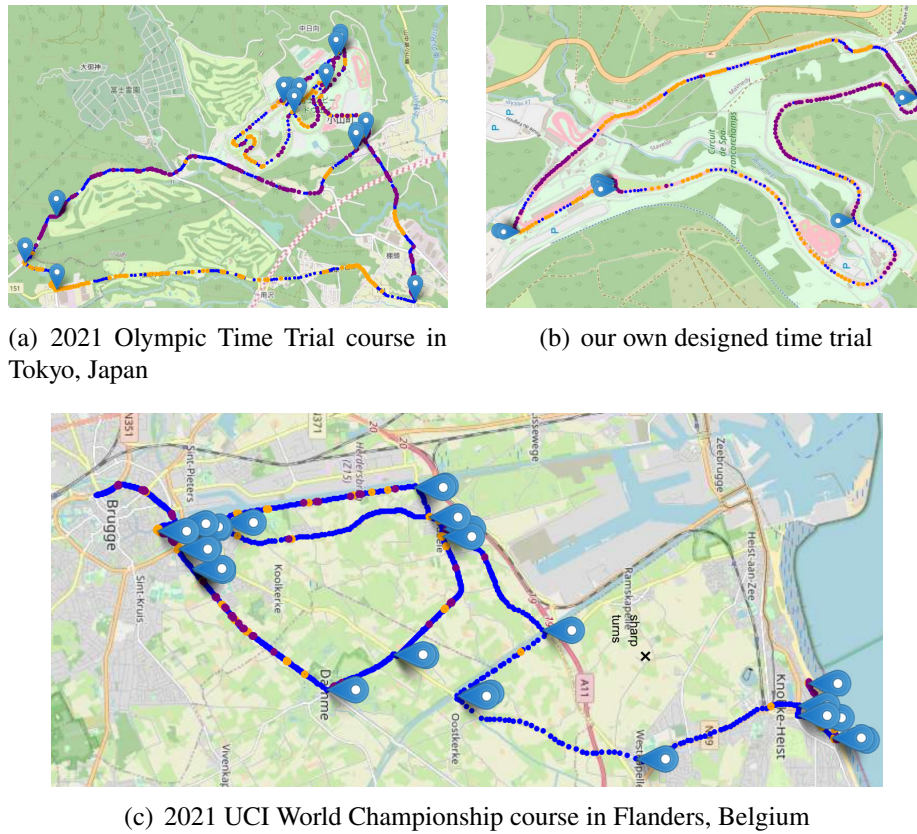


**Figure 11:** Power curve of riders' of different types and genders

**Figure 11** is the map of the above three tracks. We sample according to the track on the map, and calculate the characteristics of the track through the latitude and longitude of each sampling point. The blue points on the map represent flat roads, orange and purple represent nontrivial road grades, orange points represent uphill, purple points represent downhill, and blue markers represent sharp turns.

## 4.5 Simulation Results

We apply our models to the three circuits and obtain the results as shown in **Table 6**. As results are quite close to real race, our model is feasible. Data in **Table 6** is obtained from the **Figure 10**.

**Table 6:** Lap Time

	FUJI	UCI	our own designed course
sprinter	34.25min	67.66min	16.53min
time trial specialist	31.66min	62.47min	14.77min

## 5 Influences of Weather and Environment

### 5.1 Wind Strength and Wind Direction Influences

#### 5.1.1 Improvements of The Kinematic Bicycle Model

The external wind speed and direction mainly affect the air resistance to the bicycle. Therefore, the air resistance equation in the model is improved as follows:

$$F_w = F_{win} + F_{wex} \quad (23)$$

Due to wind speed and wind direction changes, the air resistance is calculated by the following formula:

$$F_{wex} = \frac{1}{2} C_D A \rho (u_w \cos \beta)^2 \quad (24)$$

where,  $\beta$  is the angle between the wind speed and the direction of travel at this moment.

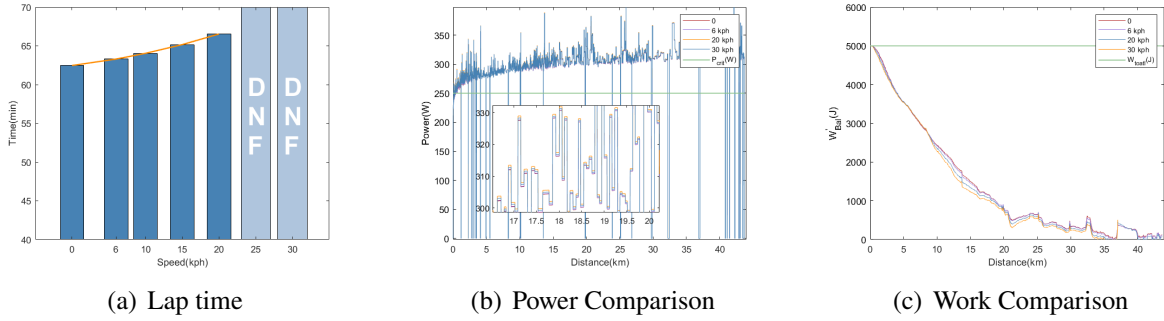
#### 5.1.2 Processing of Map Data

In Task2, we have processed and obtained the travel direction of each point. we have divided the wind direction into four, i.e. southeast, southwest, northeast, and northwest, and obtained the angle between the wind speed and the wind direction at each point by the following formula:

$$\beta = \arccos \frac{\vec{u}_x \cdot \vec{u}_w}{|\vec{u}_x| |\vec{u}_w|} \quad (25)$$

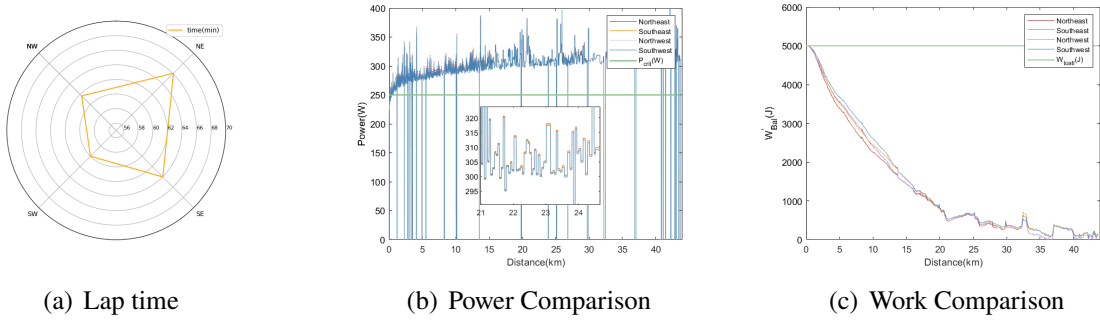
#### 5.1.3 Analysis of Results

We first fixed **the wind direction** (southeast wind) to observe the effect of wind strength on the cyclists' performance.

**Figure 12:** Analysis when wind direction is fixed

We adjusted the wind speed from 0 to 20kph and the Lap time increased from 62.47 to 66.53 minutes, and then from 20kph to 25kph and 30kph, at which point the race could not be finished according to the previous strategy. This suggests that wind speed has a large effect on the model, with the time taken to finish increasing as the wind speed increases.

We then fixed **the wind speed**(10kph) to analyze how the wind affected the cyclists' results.

**Figure 13:** Analysis when wind speed is fixed

The effect of wind direction on lap time is related to the course topography. For 2021 UCI World Championship time trial course in Flanders, Belgium, we evaluated the effect of wind direction on lap time in four directions: northeast, northwest, southeast and southwest, with the southwest wind having the shortest lap time and the northeast wind having the longest lap time. When the wind direction is changed by 25%, the lap time will change by 1.7% on average.

## 5.2 Altitude and Temperature Influences

### 5.2.1 Analysis of Influencing Factors

Here we ignore the impact of external factors on the driver's own ability, and mainly consider the influence of changes in the external physical environment. The air resistance to the rider in the process of travel is proportional to the dynamic pressure of the gas, which is related to **the windward area** and **air density** of the rider. According to the ideal gas equation of state we know that:

$$\rho = \frac{PM}{RT} \quad (26)$$

where  $P$  is atmospheric pressure,  $M$  is molar mass,  $R$  is universal gas constant,  $T$  is temperature.

We then calculated the air density at each altitude and temperature, as shown in the following tables:

**Table 7:** The relationship between  $\rho$  and Temperature

Temperature( $^{\circ}\text{C}$ )	10	15	20	25	30	35
$\rho$ ( $\text{kg}/\text{m}^3$ )	1.243	1.221	1.200	1.180	1.161	1.142

**Table 8:** The relationship between  $\rho$  and Altitude

Altitude(m)	0	1000	2000	3000
$\rho$ ( $\text{kg}/\text{m}^3$ )	1.180	1.052	0.935	0.818

## 5.2.2 Analysis of results

In terms of altitude, we have plotted the following figure to illustrate.

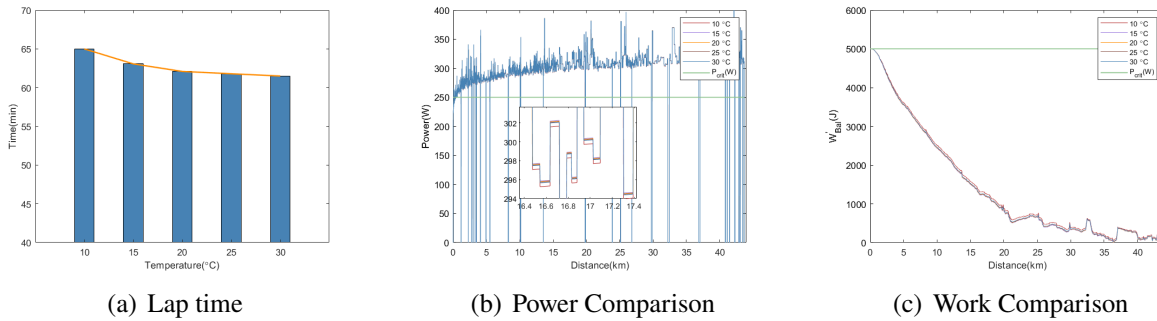


**Figure 14:** Analysis when temperature is fixed

Increasing the altitude from 0m to 3000m, the lap time was found to increase more or less linearly. For every 1000m increase in Altitude, the lap time increases by an average of 2.06 minutes.

In terms of temperature, we have plotted the following figure to illustrate.

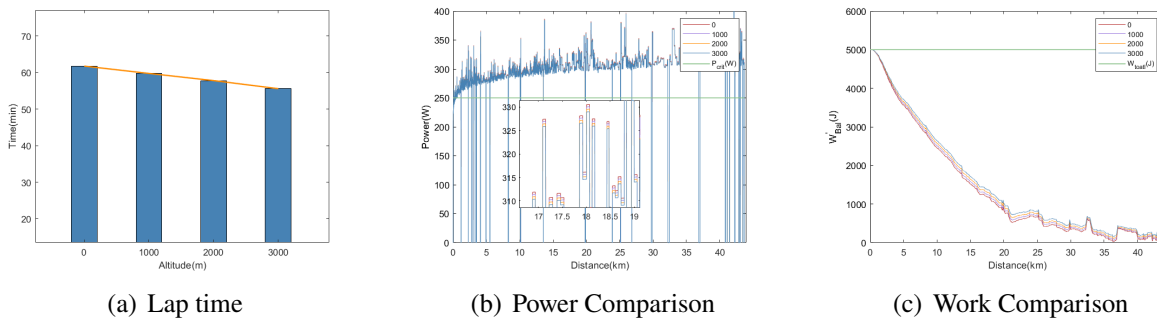


**Figure 15:** Analysis when altitude is fixed

Excluding the extremes of temperature that are unsuitable for athletes, the lap time decreases as the temperature increases. The lap time decreases from 65.2 minutes to 61.5 minutes as the temperature increases from  $10^{\circ}C$  to  $30^{\circ}C$ . Converting the temperature units to kelvins, the effect on the lap time is on average 0.88% for every 1% change in temperature from  $273.15K$ .

## 6 Sensitivity Analysis of Power Distribution Model

Since the rider cannot always follow the originally set power target, a certain amount of deviation always exists. Therefore, the corresponding sensitivity analysis of the power distribution module is required to evaluate the size of its impact.

### 6.1 Adjustments to Power Distribution Models

The overall idea of our improvement is as follows:



**Figure 16:** Control Strategy

We have added a random processing module, the principle of which is to generate a uniformly distributed random number  $rand$  from  $-0.2$  to  $+0.2$ , and its probability density function is:

$$f(x) = \begin{cases} 0, & x < -0.2 \text{ or } x > 0.2 \\ \frac{1}{0.4}, & -0.2 \leq x \leq 0.2 \end{cases} \quad (27)$$

The formula for calculating the actual output power is as follows:

$$P = P \cdot rand \quad (28)$$

### 6.2 Analysis of Results

Lap time was largely unaffected when the rider was unable to precisely control the output of power. As **Figure 17** shows, the rider spent almost the same time as before.

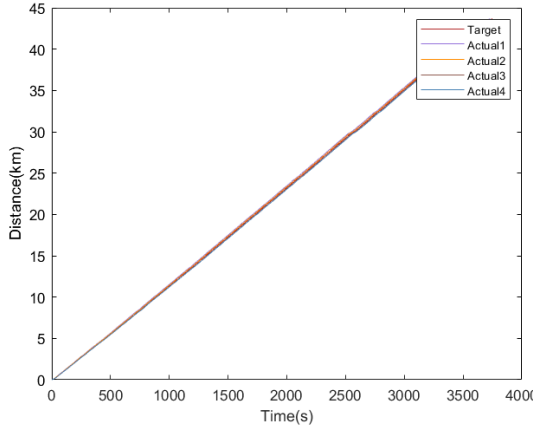


**Figure 17:** Race time with simulated fluctuations(compared to without fluctuations)

Although we have tried to increase the randomness of errors in the riders' control of power, the lap time is not increased by more than 10s. It can be assumed that the human error in energy control is negligible if the athletes subjectively follow the energy distribution model. According to our simulation result **Figure 18**, normal disruption of the track plan has few effects on the performance of the rider. That is to say, our models have excellent robustness after optimizing.

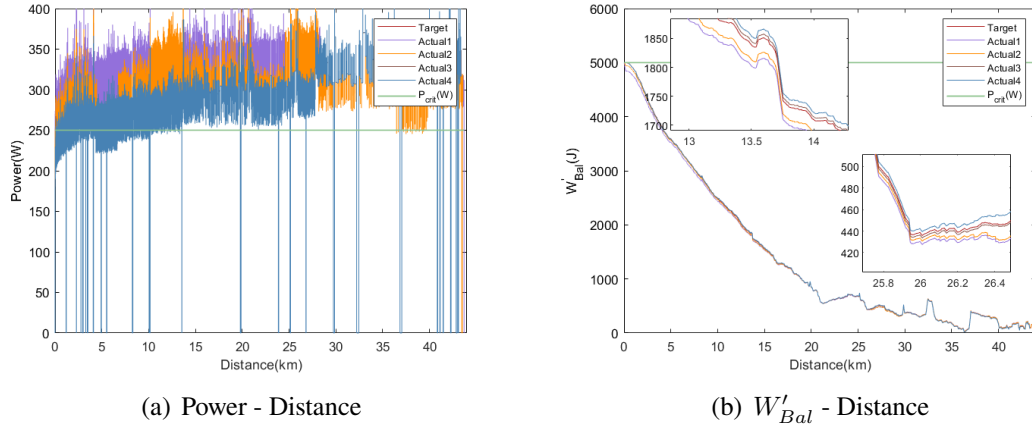


**Figure 18:** Power and  $W'_{bal}$  Comparison to no mistakes

## 7 Extension and Optimization of Our Model

In order to deal with the situation that using optimal power for a team time trial of six riders per team, we should focus on examining the competition strategy of the team road cycling time trial to improve the overall result. The team race has a total of six people, but it's worth mentioning that the race results are based on the time the fourth member crosses the finish, which gives us an idea for our strategy.

## 7.1 Discussion on Team Strategies

We checked the relevant materials and watched the video of the uci team road cycling time trial[9]. We summarize and discuss about the race as if we are the Directeur Sportif. Finally, several common strategies are obtained through our efforts.

That is,

- The six riders **take turns riding in a paceline**(namely takes turns being a wind shield for his/her teammate).
- Keep shorter **following distance**.
- The four riders who own **better ability to sprint** are chosen to finish the final sprint.

## 7.2 Optimization of Our Model

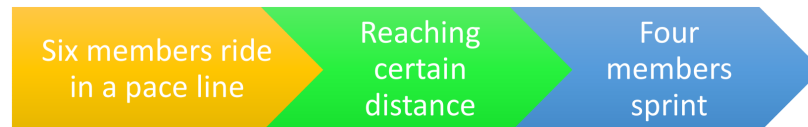
### 7.2.1 Problems about Riding in a Paceline

After consulting relevant literature on aerodynamics, the following results are obtained: with a front bicycle riding in a paceline, the air resistance received by the rear car can be reduced by 49.98% when the distance between the front and rear car is within 0.1 – 0.4m. At 1.6m, the air resistance is 60.34% of the original. And at 3.6m, the air resistance is 72.57% of the original. Therefore, we believe that it is most appropriate to keep the distance between 0.3 – 0.4m[4]. The resistance value is shown as follows.

$$F_w = 49.98\% \cdot F_w \quad (29)$$

### 7.2.2 The Selection of Optimal Parameter

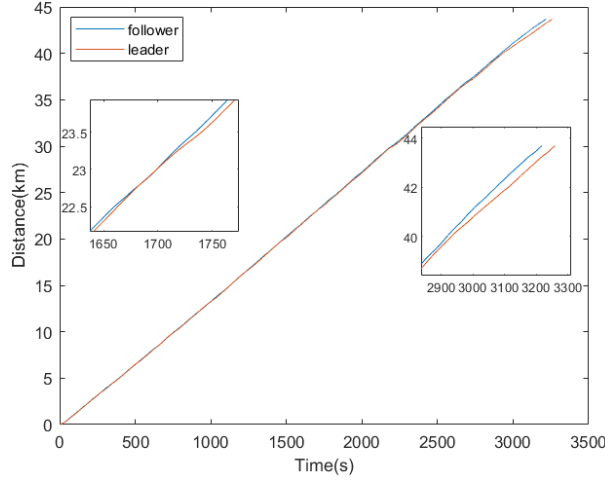
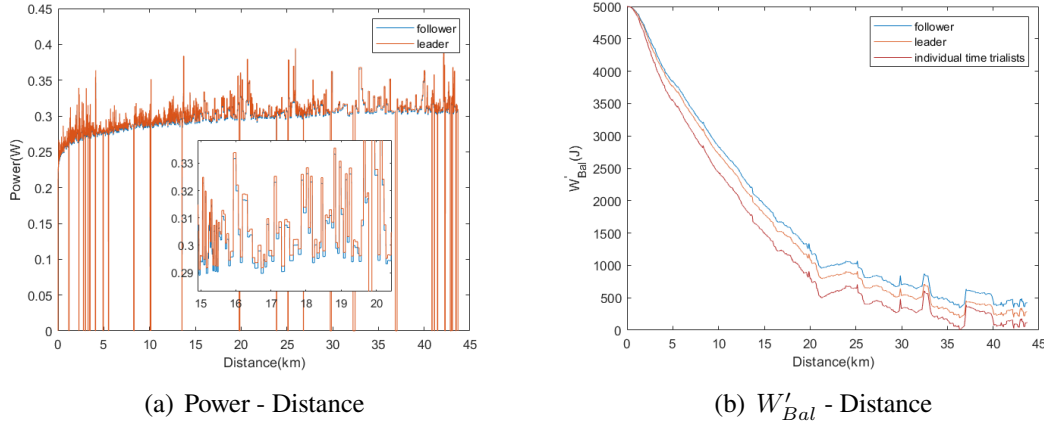
On the basis of the previous article, three new parameters  $t_{sprinter}$ ,  $t_{Leadout}$  and  $D_{sprinter}$  are added here, the first of which is the time that the sprinters ride in a paceline. The second one is the time the other two riders ride in a paceline. The third is the distance to start the sprint from the finishing line. The operation logic of the model is shown in the following figure:



**Figure 19:** The operation logic of the optimized model

## 7.3 Analysis of Results

In a team time trial race, the members work together to reduce wind resistance compared to an individual time trial, which makes the lap time shorter than an individual time trial. Before crossing the line, the leader and follower ride in a paceline, so although the leader uses more energy than the follower, the difference is not significant, as shown in **Figure 21**. The leader will use significantly more energy than the follower as he will be breaking as much wind as possible for the follower before the final line, and the follower will clearly outpace the leader near the finish, as shown in **Figure 20**. To sum up, team time trial is shown to be 530s faster than individual time trial. The final result is that ride-in-a-paceline time for the four sprinters is 25s, the other two alternate wind Time of ride-in-a-paceline are 40s, and the final sprint distance is 40km, and the total time of the team race will be about 530seconds faster compared to the individual race.

**Figure 20:** distance-time curve**Figure 21:** follower vs. leader

## 8 Strengths, Weaknesses and Further Improvements

### 8.1 Strengths

- **Realism:** Our kinematic bicycle model takes into account the forces on the vehicle as far as possible and is fully modelled and functional. In addition, our power distribution functions are based on optimization of the actual output trends of the athletes and are realistic.
- **High adaptability:** We have applied our individual time trial model to three different tracks and optimized the parameters for each of them with good and accurate results, proving its high adaptability.
- **High accuracy:** We compare our results with the actual results and the difference between them is small, thus proving that the parameters optimized by our PSO algorithm are accurate.
- **Robustness:** We fluctuate the power curve over a range by introducing uniformly distributed random numbers and the results show little difference in total time spent, proving that the system is robust and

athlete-friendly.

- **Highly scalable:** Our model can be applied to team time trial races with some tuning and we have also optimized its parameters and the results show that it still works, demonstrating its potential to be further extended to more niche areas of cycling.

## 8.2 Weaknesses and Further Improvements

Because of the high stiffness of the kinematic bicycle model, the time required for optimization is long and the number of iterations of our PSO algorithm is limited with computational resources to determine whether the optimization parameters are optimal. Also some parameters related to the bicycle are difficult to obtain and can only be estimated.

Further parameter optimization can be carried out later if stronger computational resources are available to confirm that the parameters are globally optimal solutions. In the meantime the bicycle can be subjected to aerodynamic tests in a wind tunnel and other relevant tests to obtain complete and reliable parameter values.

## References

- [1] Springer,Alexander D.Optimizing cycling power. Massachusetts Institute of Technology, 2016. Web. 21 Feb. 2022.
- [2] Zhisheng Yu, Qunsheng Xia, Liuqi Zhao, Jingguang Lun, Weixin Liu, Jiangang Sun, Keqiang Li, and Xuewu Ji. *Auto Theory*,5th ed.Beijing: China Machine Press,1981. Web. 21 Feb. 2022.
- [3] Skiba, Philip Friere, and David C. Clarke. "*The W' Balance Model: Mathematical and Methodological Considerations*". International Journal of Sports Physiology and Performance 16.11 (2021): 1561-1572. <https://doi.org/10.1123/ijspp.2021-0205>. Web. 21 Feb. 2022.
- [4] Liying Jin."*Impact of aerodynamics on track cycling*"[J].Sports Science and Technology Literature Bulletin,2005(05):45. Web. 21 Feb. 2022.
- [5] Jos J. de Koning, Maarten F. Bobbert, Carl Foster. *Determination of optimal pacing strategy in track cycling with an energy flow model*. In : Journal of Science and Medicine in Sport (1999), pp. 266-277. issn: 1440-2440. Web. 21 Feb. 2022.
- [6] Gordon, S. *Optimising distribution of power during a cycling time trial*. Sports Eng 8, 81-90 (2005). DOI: <https://doi.org/10.1007/BF02844006>. Web. 19 Feb. 2022.
- [7] Skiba, Philip F, et al. "*Modeling the Expenditure and Reconstitution of Work Capacity above Critical Power.*" American College of Sports Medicine (2012): 1526-1532. Web. 21 Feb. 2022.
- [8] Information on <https://www.la-flamme-rouge.eu/>. Web. 19 Feb. 2022.
- [9] Information on <https://www.trainingpeaks.com/>. Web. 18 Feb. 2022.
- [10] Race Videos on <https://www.uci.org/watch-uci-events/>. Web. 21 Feb. 2022.
- [11] Passfeld L et.al. 2017. *Knowledge is power: issues of measuring training and performance in cycling*. J Sports Sci 35(14):1426-1434. Web. 21 Feb. 2022.
- [12] van Erp T, de Koning JJ. 2019. *Intensity and load characteristics of professional road cycling: differences between men's and women's races*. Int J Sports Physiol Perform 14(3):296-302. 21 Feb. 2022.

- [13] Muriel X et.al. 2021. *Physical demands and performance indicators in male professional cyclists during a grand tour: worldtour versus proteam category.* Int J Sports Physiol Perform 1(aop):1-9 Nicolò A, Bazzucchi I, Sacchetti M (2017) Parameters of the 3-mi. Web. 21 Feb. 2022.
- [14] Menaspà P et.al. 2015. Physical demands of sprinting in professional road cycling. Int J Sport Nutr Exerc Metab 36(13):1058-1062 Web. 21 Feb. 2022.

## Race Guidance

this is document